A Letters Journal Exploring the Frontiers of Physics

February 2010

EPL, **89** (2010) 44001
doi: 10.1209/0295-5075/89/44001

www.epljournal.org

Nanoflows through disordered media: A joint lattice Boltzmann and molecular dynamics investigation

J. Russo[1(a)], J. Horbach[2], F. Sciortino[1] and S. Succi[3,4]

[1] *Dipartimento di Fisica and CNR-INFM-SOFT, Università di Roma La Sapienza - Piazzale A. Moro 2, 00185 Roma, Italy, EU*
[2] *Institut für Materialphysik im Weltraum, Deutsches Zentrum für Luft- und Raumfahrt (DLR) 51170 Köln, Germany, EU*
[3] *Istituto Applicazioni Calcolo, CNR - via dei Taurini 19, 00185 Roma, Italy, EU*
[4] *Freiburg Institute for Advanced Studies, Albert Ludwig University - Albertstrasse 19, 79104 Freiburg, Germany, EU*

received 10 September 2009; accepted in final form 8 February 2010
published online 8 March 2010

PACS 47.56.+r – Flows through porous media
PACS 47.11.-j – Computational methods in fluid dynamics
PACS 47.61.-k – Micro- and nano- scale flow phenomena

Abstract – We investigate nanoflows through dilute disordered media by means of joint lattice Boltzmann (LB) and molecular dynamics (MD) simulations —when the size of the obstacles is comparable to the size of the flowing particles— for randomly located spheres and for a correlated particle-gel. In both cases at sufficiently low solid fraction, $\Phi < 0.01$, LB and MD provide similar values of the permeability. However, for $\Phi > 0.01$, MD shows that molecular-size effects lead to a decrease of the permeability, as compared to the Navier-Stokes predictions. For gels, the simulations highlights a surplus of permeability, which can be accommodated within a rescaling of the effective radius of the gel monomers.

Introduction. – Flow phenomena in disordered media are a subject of great theoretical and practical interest [1,2]. In case of a fluid streaming through a random, low-density porous matrix, descriptions based on continuum hydrodynamics have been provided [3–8]. Continuum theories are expected to hold on macroscopic scales and thus might be non-applicable to fluid flow through microfluidic devices or through micro-gel matrices where the typical size of the pores is at nanometer length scales and below.

However, as shown in several simulation studies (see, *e.g.*, refs. [9,10]), hydrodynamics often holds down to the molecular scale, as far as simple steady-state flows of dense liquids are concerned. Similar conclusions have also been reached recently for the non-trivial case of microflows over super-hydrophobic surfaces [11]. However, in particular for the case of nanoflow in disordered media, the question of whether/to what extent continuum theory is applicable to flows at the nanoscale in porous materials, remains open to this day. Indeed, previous studies on flow phenomena in disordered media have employed only mesoscopic or macroscopic simulation methods, such as finite-element schemes [12,13], the LB method [14–21], and smoothed particle dynamics [22,23]. In this work, we address such a question using a combination of lattice Boltzmann (LB) and molecular dynamics (MD) simulations. While LB is used as an effective Navier-Stokes equation solver, the MD simulations are performed to solve Newton's equations of motion for a three-dimensional system of soft spheres. As porous media, we consider non-overlapping random arrangements of particles, as well as particle gel networks at different packing fractions. In both cases, flows through bulk porous media and through porous media confined between parallel plates are considered. First, we show that a *quantitative* mapping between LB and MD can be established. Second, we study to what extent continuum theory is applicable at the molecular scale. This is particularly interesting for gel networks, since they introduce long-ranged structural correlations which are not present in the random arrangement of obstacles. For this case, we quantify deviations to predictions of the theory. Interestingly, the theory is renormalizable, *i.e.* the observed deviations due to an excess of permeability can be reabsorbed within a readjustment of the effective radius of the gel monomers.

(a) E-mail: john.russo@roma1.infn.it

Theory. – For low-Reynolds-number flow, Darcy [24] first established empirically a linear relation between the average volumetric flow velocity through unit cross-sectional area, $\langle\vec{v}\rangle$, and the pressure gradient $\vec{\nabla}p$ of the fluid across the porous medium, $\langle\vec{v}\rangle = -(k/\eta)\vec{\nabla}p$ (with η the shear viscosity of the fluid and k the permeability). Note that the measurement or calculation of $\langle\vec{v}\rangle$ implies an average over different realizations of the porous medium. In case of high dilution of spheres of radius R as a porous medium, Darcy's law reduces essentially to Stokes' law, with a permeability $k_0 = 2R^2/9\phi$, [16,25].

Brinkman's theory is based on the stationary Navier-Stokes equations [25], $\eta\nabla^2\vec{v} - \vec{\nabla}p + \vec{F} = 0$ and $\vec{\nabla}\cdot\vec{v} = 0$, with $\vec{v}$ the flow velocity and $\vec{F}$ an external force per unit volume acting on the fluid. By setting $\vec{v} \equiv \langle\vec{v}\rangle$ and by expressing the external force $\vec{F}$ through Darcy's law, $\vec{F} = -\eta\vec{v}/k$, Brinkman's equation of motion [3] is obtained:

$$\nabla^2\vec{v} - \frac{1}{\eta}\vec{\nabla}p - \frac{1}{k}\vec{v} = 0. \tag{1}$$

This equation describes the porous matrix as an effective medium that exerts a friction on the fluid. The substitution of the external force $\vec{F}$ by Darcy's law is expected to be valid only if the packing fraction of the porous medium is sufficiently small (see below).

From eq. (1), one can derive an explicit formula for the flow between two parallel plates in presence of a porous medium. Consider a gravitational force field ρg in the x-direction and two parallel plates at $z = -L/2$ and $z = L/2$. The porous medium between the plates is represented by a random matrix of fixed non-overlapping spheres. Then, the velocity profile is given by

$$v_x(z) = \frac{kg}{\nu}\left[1 - \frac{\cosh(z/\sqrt{k})}{\cosh(L/2\sqrt{k})}\right] \tag{2}$$

with $\nu = \eta/\rho$ the kinematic velocity of the fluid.

For a dilute collection of non-overlapping spheres, different expressions for the permeabiliy as a function of the volume fraction, $\Phi \equiv 4\pi R^3 n/3$, of the porous medium have been investigated [3–7]. A simple expression for the permeability over the entire range of volume fractions has been proposed by van der Hoef *et al.* [7] by fitting both LB [5,7] and multipole expansion data [6]:

$$k = k_0\left[10\frac{\Phi}{(1-\Phi)^3} + (1-\Phi)\left(1 + 1.5\sqrt{\Phi}\right)\right]^{-1}. \tag{3}$$

Note that the square-root of the permeability, $\sqrt{k}$, describes the screening length of the flow field due to the interaction with the porous medium.

Equations (2) and (3) are the main results which our simulations on nanoscopic scales will be compared against.

Methods and simulation details. – We use a standard lattice Boltzmann model with single-step relaxation term [26–28]. No-slip boundary conditions at solid surfaces are implemented via standard bounce-back collision rules [29]. Fully developed periodic flows are generated by pressure boundary conditions [30]. The size of the LB D3Q19 lattice is $(192 \times 48 \times 48)$ in lattice units. When present, slit walls are placed parallel to the xy-plane with surfaces at locations $z = 4$ and $z = 43$.

For the MD fluid, we choose a binary model system as proposed by Hedges *et al.* [31] for which, also at low temperatures, crystallization is not a problem and thus this model can be used in forthcoming studies on glass-forming fluids in porous media.

The MD fluid is composed of a 50:50 mixture of A- and B-type particles interacting with a WCA potential, $V_{\alpha\beta}(r) = \{4\epsilon_{\alpha\beta}[(r/\sigma_{\alpha\beta})^{-12} - (r/\sigma_{\alpha\beta})^{-6}] + \epsilon_{\alpha\beta}\}$, for $r < r_- = 2^{1/6}\sigma_{\alpha\beta}$ (zero else). The parameters are $\epsilon_{\rm AA} = \epsilon_{\rm AB} = \epsilon_{\rm BB} = 1$ and $\sigma_{\rm AA} = 1.0$, $\sigma_{\rm AB} = 11/12$, $\sigma_{\rm BB} = 5/6$ [31]. In the following, length and energy scales are measured in units of $\sigma = \sigma_{\rm AA}$ and $\epsilon = \epsilon_{\rm AA}$, respectively; temperature is in units of the potential depth ϵ. The masses of both A and B particles are taken equal, $m = m_{\rm A} = m_{\rm B} = 1$. The equations of motion are integrated with the velocity form of the Verlet algorithm using a time step $\delta t = 10^{-3}$ in units of $t_0 = [m\sigma^2/\epsilon]^{1/2}$. Thermalization at the constant temperature $T = 5.0$ is obtained with a Lowe thermostat [32], which provides local momentum conservation and thus it preserves the correct hydrodynamic behavior of the fluid. The size of the MD simulation box is $(32 \times 8 \times 8)$ in units of σ. The total density of all systems is set to $\rho = 1.3$. First the porous material is introduced in the simulation box which is then filled with the appropriate number of fluid particles to reach the desired density. A pressure drop is applied along the x direction by adding a gravitational field (g) on the fluid particles, whose intensity (g in units of σ/t_0^2) is chosen such that a linear response of the system is provided. The kinematic viscosity ν of the fluid has been calculated aside from separate Poiseuille-flow simulations, which yields $\nu = 24\,\sigma^2/t_0$.

The porous material is composed of A-type particles and their position is kept fixed as a momentum absorbing material.

To simulate slit walls (whenever present), the system is first equilibrated in a $(32 \times 8 \times 10.2)\,\sigma$ box and then all fluid particles within a distance $z_w = 1.2\sigma$ from the planes $z = 0$ and $z = 10.2\sigma$, are labelled as wall particles. Wall particles retain the same interactions as fluid particles, but their position is kept fixed. In this way we account for the walls roughness and avoid layering effects. To avoid diffusion of fluid particles in the wall region, an external potential (previously defined as $V_{\rm AA}$) is added along two planes parallel to the xy-plane, at a distance $z_p = 2^{1/6}\sigma$ from the slit walls. In this way, fluid particles feel the external potential only when they start diffusing into the walls.

To compare LB and MD, units have to be scaled appropriately. One of our goals is to assess the validity of the LB predictions for microscopic flows which can be

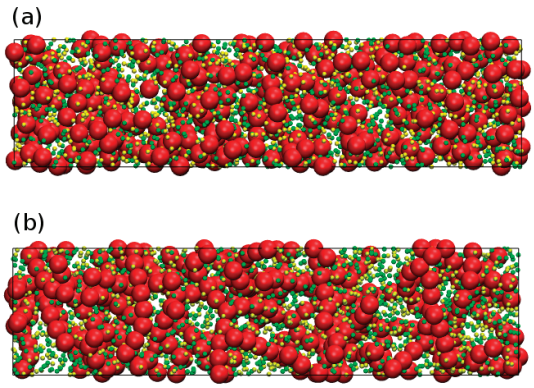

Fig. 1: (Colour on-line) Two snapshots at $\Phi = 0.1$ with random medium (a) and gel (b). Porous media are coded in red, the binary mixture fluid is coded in yellow and green. The size of the fluid particles is not at scale to improve visibility.

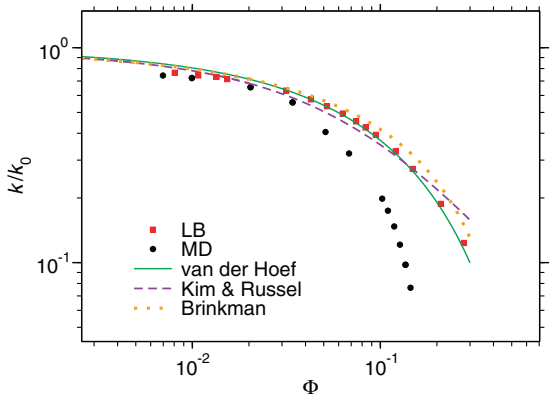

Fig. 2: (Colour on-line) Dimensionless permeability as a function of volume fraction Φ for the random sphere matrix from MD simulations (circles) and LB simulations (squares). The LB data is well described by the theoretical prediction of eq. (3) (continuous line), except at low volume fractions where the agreement holds with the asymptotically exact result of Kim and Russel [4] (dashed line). For comparison also the result of the Brinkman theory [3] (dotted line) is shown. MD results consistently deviate from hydrodynamic predictions for $\Phi > 0.01$.

resolved through MD. As shown recently [10], in order to recover quantitative agreement with MD results, the LB simulation must be taken down to microscopic resolution, *i.e.* fractions of the range of molecular interactions. The space conversion proceeds as follows. In LB simulations the lattice spacing, Δx is set to unity, while in MD simulations the unit of length is fixed by the parameter σ. To resolve fractions of the interaction potential we set $\Delta x < \sigma$, specifically we choose $\sigma = 6\Delta x$. This fixes the conversion of space units. It also fixes the radius of the LB spheres as $R = \sigma/2 = 3\Delta x$. In the rest of the letter we adopt $\sigma = \sigma_{\rm AA} = 1$ as our unit of length.

The time conversion is determined from kinematic viscosity ν. The kinematic viscosity in the LB simulation is given by $\nu_{\rm LB} = \widetilde{\nu}_{\rm LB}\frac{\Delta x^2}{\Delta t_{\rm LB}}$, with $\widetilde{\nu}_{\rm LB} = 1/6$, while for MD we have $\nu_{\rm MD} = \widetilde{\nu}_{\rm MD}\frac{\sigma_{\rm AA}^2}{\Delta t_{\rm MD}}$, with $\widetilde{\nu}_{\rm MD}$ given by the Poisseuille flow comparison. By imposing $\nu_{\rm LB} = \nu_{\rm MD}$ and remembering the space conversion factor we obtain for time scales $\Delta t_{\rm MD} = \frac{\Delta t_{\rm LB}}{6^2}\frac{\widetilde{\nu}_{\rm MD}}{\widetilde{\nu}_{\rm LB}}$.

The Reynolds number is $Re = \langle\vec{v}\rangle R/\nu$, where $\langle\vec{v}\rangle$ is the spatially averaged velocity, R is the radius of the obstacles and ν is the kinematic viscosity. We use very low external fields ($g = 0.05$ in units of $\sigma/\Delta t_{\rm MD}^2$), so that $Re < 10^{-3}$ and simulations can be considered under effectively zero-Reynolds-number conditions.

MD and LB simulations are best compared in terms of dimensionless quantities, such as the normalized permeability k/k_0, where k_0 is the permeability of a single sphere (as given by Stokes law). Other dimensionless quantities used in the present work are the dimensionless position z/L, with L the width of the slit, and the dimensionless velocity profile $u = \nu v/(gR^2)$.

Simulations of fluid flow through two types of obstacles are considered: random media and gel media.

Random media are modeled as a collection of non-overlapping spheres of radius R. We average over 50 independent random configuration for each volume fraction Φ considered, in the range $\Phi = 0.008$–0.27.

Gel networks are characteristic random structures with long-range spatial correlations. A gel is usually made of a network of polymer strands or from self-assembled colloidal particles. The number of bonds is so high that it is always possible to move from one gel-forming monomer to another without ever leaving the network. This interlinked structure confers the gel its peculiar properties, sharing characteristics of both liquids and solids. It behaves like a liquid since it can be made up primarily of fluid and allow both diffusive and convective transport through its volume. On the other hand, a gel is also able to support a shear stress and behave elastically, acting like a solid. In the present study, we neglect the elastic behaviour of gels, keeping the monomers fixed and taking advantage of the rigid framework through which mass transport can occur. Gel structures are obtained through equilibrium MD simulations of Patchy particles. Patchy particles are a class of short-ranged valence-limited particles which can reach low temperatures without encountering the gas-liquid phase separation [33]. The corresponding low-T arrested states are in fact equilibrium gels which we use for the present study. We follow the procedure described in [34], for networks with average valence 2.25, equilibrated until all particles belong to the same spanning cluster. Here, we generated 50 independent gel configurations at each of the packing fractions $\Phi = 0.03$, 0.05, 0.075, 0.1, 0.15, and 0.2. Figure 1 shows snapshots of MD configurations with the random medium (a) and the gel (b) at $\Phi = 0.1$.

Results. – All obstacles considered in the present paper are collections of spheres whose hydrodynamic radius is estimated by measuring the drag force on a single sphere with periodic boundary conditions and

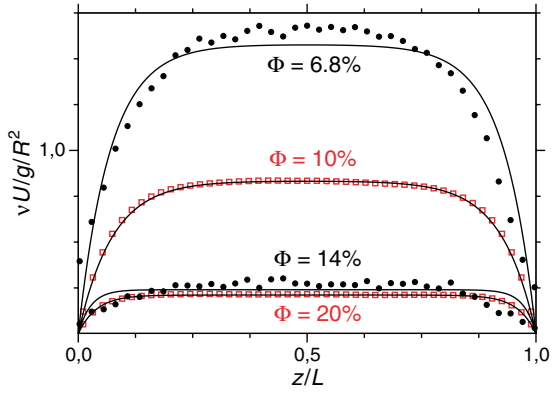

Fig. 3: (Colour on-line) Comparison of LB (squares) and MD (circles) for the random medium at different volume fractions. Full lines are the theoretical profiles, eq. (2). Agreement between LB data and theoretical predictions is perfect for all volume fractions investigated. MD solutions display instead a different pattern.

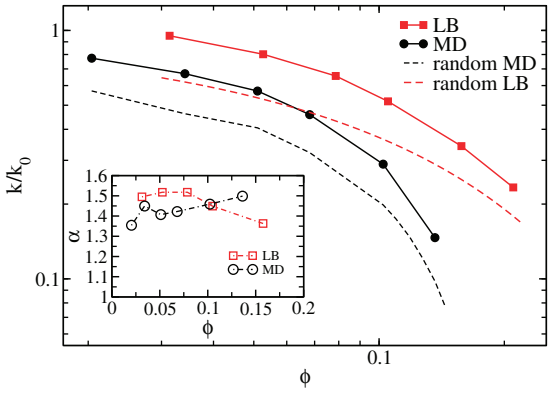

Fig. 4: (Colour on-line) Dimensionless permeability as a function of volume fraction Φ for the gel matrix from MD simulations (circles) and LB simulations (squares). The dashed line represents the results for the random sphere matrix from fig. 2. The inset shows the α parameter defined in eq. (4) for MD (circles) and LB (squares).

comparing the result with the theoretical expression given by Hashimoto [35]. For LB, this procedure leads to a hydrodynamic radius of $R = 3.05$, slighty larger than the nominal radius (in agreement with previous studies [29]). For MD we obtain a value of $R = 0.44$, assuming slip boundary conditions. The same value, $R = 0.44$ can be estimated from the interaction potential for the MD particles: at $2 \cdot R = 0.88$ the potential energy between two particles, separated by a distance $2 \cdot R = 0.88$, is approximately equal to $k_B T$. We conclude that for our atomistic fluid slip boundary conditions provide a consistent description of the interactions between obstacles and fluid particles. We remind that the difference between stick and slip boundary conditions is included in the Stokes expression: $k_0 = 2R^2/(9\Phi)$ (stick) and $k_0 = R^2/(3\Phi)$ (slip).

Figure 2 shows the results for the flow through random porous media (without slit walls) for both MD and LB simulations. LB results confirm eq. (3), except for the lowest volume fractions, where the low-density result of result of Kim and Russel [4] holds. Note that the agreement with Brinkman theory is also good for low volume fractions, say $\Phi < 0.08$. The grid-independence of LB results was checked by doubling the resolution ($\sigma = 12\,\Delta x$). MD data shows instead significant deviations from the hydrodynamic solution. While for $\Phi < 0.01$ the agreement between MD and LB seems to hold (within statistical accuracy), at higher volume fractions the MD results show visible under-deviations. These can be interpreted as genuine atomistic effects, where the reduced permeability is due to the finite size of the molecules. Indeed, at $\Phi = 0.01$, the ratio d/σ between the average intermolecular distance and the molecular effective diameter is of the order of $d/\sigma \sim 4$, whereas for $\Phi = 0.1$, one has $d/\sigma \sim 2$.

We have also investigated the effect of slit walls on the permeability k. To this end, we have determined the velocity profiles $v_x(z)$, averaged over all crossflow yz sections. Inspection of the LB and MD velocity profiles in fig. 3 for random media at different values of Φ shows excellent agreement with the prediction of eq. (2) for LB. In contrast to that, the MD profiles show a different pattern from the hydrodynamic solution: again, this indicates the differences between hydrodynamic and atomistic flow for $\Phi > 0.01$.

We can conclude that both global (permeability) and local (velocity profiles) properties of an atomistic flow show consistent deviations from the hydrodynamic solution also at relatively low volume fractions. The results obtained show the limits of applicability of continuum approaches when dealing with microscopic and structured fluids.

We now turn to the study of the effects of the correlation between the obstacles' positions on the flow properties for both the hydrodynamic solution (LB) and the microscopic flow (MD). Differently from random spheres, gel media is characterized by short-range correlations between the particles' positions. Figure 4 reports the results for the gel media for both MD and LB simulations. This figure indicates that the permeability of the gel is always higher than that of the random media for both hydrodynamic and microscopic flows. Also for the gel, the MD permeability always underestimates the LB solution at packing fractions $\Phi > 0.01$.

Next, we show that the increased permeability induced by the correlations between the obstacle particles can be taken into account by simple renormalization of the theory for random obstacles. We first observe that the permeability can be formally written as $k = R^2 f(\Phi)$, where $f(\Phi)$ is a dimensionless function of Φ. Given the proper expression for the random sphere case (eq. (3) for the LB data), a formal generalization for the gel case can be obtained by introducing an effective parameter $\alpha(\Phi)$,

$$k = \alpha(\Phi) R^2 f(\Phi). \tag{4}$$

The introduction of the parameter $\alpha(\Phi)$ formally corresponds to the definition of an effective Stokes radius, $R_{\rm eff}(\Phi) = \sqrt{\alpha}R$, which depends on density. The inset of fig. 2 shows the value of the parameter α calculated both for LB (squares) and MD (circles) simulations. For both types of simulations the effective Stokes radius remains almost constant at all considered volume fractions, so that we can conclude that the gel structure results in an increase of the bare permeability by about 50%, which can be also interpreted as an increase of the effective Stokes radius by a factor 1.25.

Summary and conclusions. – We have investigated nanoflows through disordered media by means of joint LB and MD simulations. For random media at $\Phi < 0.01$, both LB and MD provide similar values of the permeability, confirming that the hydrodynamic approach holds down to the nanoscale at sufficiently low volume fractions. For higher volume fractions, the MD simulations reveal under-departures from the hydrodynamic solution. Since LB simulations still agree with the eq. (3) prediction, these under-departures are most naturally interpreted as genuine atomistic effects, *i.e.* breakdown of the continuum hydrodynamic hypothesis at the nanoscale. The same conclusions result from the study of the velocity profiles within solid slabs filled with random media, showing that the MD flow is qualitatively different from LB predictions. We have then explored the effects of the correlations in the obstacles positions by studying the flow through a correlated medium, *i.e.* gels. We have shown that gels exhibit a surplus of permeability. This surplus, about 50%, can be reinterpreted as an increase of the effective radius of the gel monomers, thereby indicating that, at least for the cases explored in this work, the hydrodynamic solution appears to be renormalizable.

* * *

We thank A. Griesche for a critical reading of the manuscript. JR and FS acknowledge support from ERC 226207. JH thanks University of Roma La Sapienza for a visiting professorship.

REFERENCES

[1] Vafai K. (Editor), *Handbook of Porous Media* (Dekker, New York) 2000.
[2] Sahimi M., *Rev. Mod. Phys.*, **65** (1993) 1393.
[3] Brinkman H. C., *Appl. Sci. Res. A*, **1** (1947) 27.
[4] Kim S. and Russel W. B., *J. Fluid Mech.*, **154** (1985) 269.
[5] Ladd A. J. C., *J. Chem. Phys.*, **93** (1990) 3484.
[6] Hill R. J., Koch D. L. and Ladd A. J. C., *J. Fluid Mech.*, **448** (2001) 243.
[7] van der Hoef M. A., Beetstra R. and Kuipers J. A. M., *J. Fluid Mech.*, **528** (2005) 233.
[8] Warren P. B. and Stepanek F., *Phys. Rev. Lett.*, **100** (2008) 084501.
[9] Rapaport D. C. and Clementi E., *Phys. Rev. Lett.*, **57** (1986) 695.
[10] Horbach J. and Succi S., *Phys. Rev. Lett.*, **96** (2006) 224503.
[11] Sbragaglia M., Benzi R., Biferale L., Succi S. and Toschi F., *Phys. Rev. Lett.*, **97** (2006) 204503.
[12] Cao J. and Kitanidis P. K., *Adv. Water Resour.*, **22** (1998) 17.
[13] Andrade J. S., Araujo A. D., Buldyrev S. V., Havlin S. and Stanley H. E., *Phys. Rev. E*, **63** (2001) 051403.
[14] Succi S., Foti E. and Higuera F., *Europhys. Lett.*, **10** (1989) 433.
[15] Koponen A., Kandhai D., Hellen E., Alava M., Hoekstra A., Kataja M., Niskanen K., Sloot P. and Timonen J., *Phys. Rev. Lett.*, **80** (1998) 716.
[16] Cancelliere A., Chang C., Foti E., Rothman D. H. and Succi S., *Phys. Fluids*, (1990) 2085.
[17] Cali A., Succi S., Cancelliere A., Benzi R. and Gramignani M., *Phys. Rev. A*, **45** (1992) 5771.
[18] Spaid M. A. A. and Phelan F. R., *Phys. Fluids*, **9** (1997) 2468.
[19] Manwart C., Aaltosalmi U., Koponen A., Hilfer R. and Timonen J., *Phys. Rev. E*, **66** (2002) 016702.
[20] Capuani F., Frenkel D. and Lowe C. P., *Phys. Rev. E*, **67** (2003) 056306.
[21] Yiotis A. G., Psihogios J., Kainourgiakis M. E., Papaioannou A. and Stubos A. K., *Colloids Surf. A*, **300** (2007) 35.
[22] Jiang F. and Sousa A. C. M., *Transp. Porous Media*, **75** (2008) 17.
[23] Vakilha M. and Manzari M. T., *Transp. Porous Media*, **74** (2008) 331.
[24] Darcy H. P. G., *Les fontanes publiques de la ville de Dijon* (Dalmont, Paris) 1856.
[25] Landau L. D. and Lifshitz E. M., *Fluid Mechanics* (Pergamon, New York) 1959.
[26] Benzi R., Succi S. and Vergassola M., *Phys. Rep.*, **222** (1992) 145.
[27] Chen S. and Doolen G., *Annu. Rev. Fluid Mech.*, **30** (1998) 329.
[28] Succi S., *The Lattice Boltzmann Equation* (Oxford University Press, Oxford) 2001.
[29] Ladd A. J. C., *J. Fluid Mech.*, **271** (1994) 285.
[30] Zhang J. and Kwok D. Y., *Phys. Rev. E*, **73** (2006) 047702.
[31] Hedges L. O., Maibaum L., Chandler D. and Garrahan J. P., *J. Chem. Phys.*, **127** (2007) 211101.
[32] Lowe C. P., *Europhys. Lett.*, **47** (1999) 145.
[33] Bianchi E., Largo J., Tartaglia P., Zaccarelli E. and Sciortino F., *Phys. Rev. Lett.*, **97** (2006) 168301.
[34] Russo J., Tartaglia P. and Sciortino F., *J. Chem. Phys.*, **131** (2009) 014504.
[35] Hasimoto H., *J. Fluid Mech.*, **5** (1959) 317.